Determination of a methodology for the fatigue strength evaluation of transverse hatch coaming stays on container ships

Yann Quéméner[1], Chi-Fang Lee[1*], Po-Kai Liao[1], Kuan-Chen Chen[1], Ya-Jung Lee[2]

[1] Research Dept., CR Classification Society, Taipei, Taiwan (ROC)
[2] Department of Engineering Science and Ocean Engineering, National Taiwan University, Taipei, Taiwan (ROC)
[*]Corresponding author: chifang@crclass.org

Abstract. This study evaluated the fatigue strengthening of the foremost transverse hatch coaming stays of 6 sister container vessels of 2650 TEU capacity that suffered fatigue cracking after 1.0 year operation on a North Pacific route. For that, a simplified method was proposed to validate the fatigue strengthening by providing a target hot spot stress reduction factor as a function of the ship lifetime at the crack occurrence. Afterwards, further seakeeping and structural analyses enabled conducting the spectral fatigue analyses of the considered stays' original and strengthened designs and, by then, to validate the fatigue strengthening of the stays and the simplified approach. The fatigue driving loads, as well as the effect of the long-term operational profiles uncertainties on the fatigue were also discussed on the basis of the spectral fatigue analyses. Finally, crack growth analyses confirmed the criticality of the examined stays with regards to rapid fatigue cracking when the fatigue damage is not properly considered at the design stage.

Keywords: container ship, transverse hatch coaming, fatigue.

1 Introduction

To fit the maximum of 'boxes' in their holds, the container ships include numerous structural discontinuities that result in as much hot spot areas prone to fatigue cracking. Therefore, for all structural details referenced as critical, Class rules provide fabrication standards and specific fatigue life assessment methodologies, so that the fatigue can be properly considered at the design stage. However, fatigue cracking in container ships is still an issue to be tackled that requires the continuous development of the design and fabrication methods. Recently, significant research efforts focusing on large container vessels are put on quantifying the influence of the springing and whipping phenomena on the fatigue. Besides, researchers are also addressing the issue of relieving the uncertainties with regards to long term operational profile, e.g. operation area, loading conditions and associated routing under weather and operation constraints.

This study considered the case of 6 sister vessels of 2650 TEU capacity in which, despite an extensive fatigue life evaluation at the design stage, cracks appeared early

in their operational life and propagated rapidly in the foremost bays' transverse hatch coamings stays L2 to L11 at Fr.206 and L2 to L8 at Fr.210. Fig. 1 shows an overview of the cracked stays locations in the vessel. The ship-owner reported that, for all of the 6 vessels, the cracking appeared 1.0 year after the beginning of their operations on the North Pacific route from Taipei to Los Angeles and resulted in crack length ranging between 50 mm to 350 mm when detected by the crew. Besides, waiting for the stays upgrade on the yet uncracked vessels, the crews kept a close watch on those critical areas and reported that some previously undetected cracks appeared and propagated extensively in the stays after a voyage with particularly adverse weather conditions. Based on those observations, this study proposed a method to validate the fatigue strengthening of new stays and examined the crack initiation by damage accumulation and the subsequent crack propagation through advanced numerical methods involving seakeeping and finite element analyses.

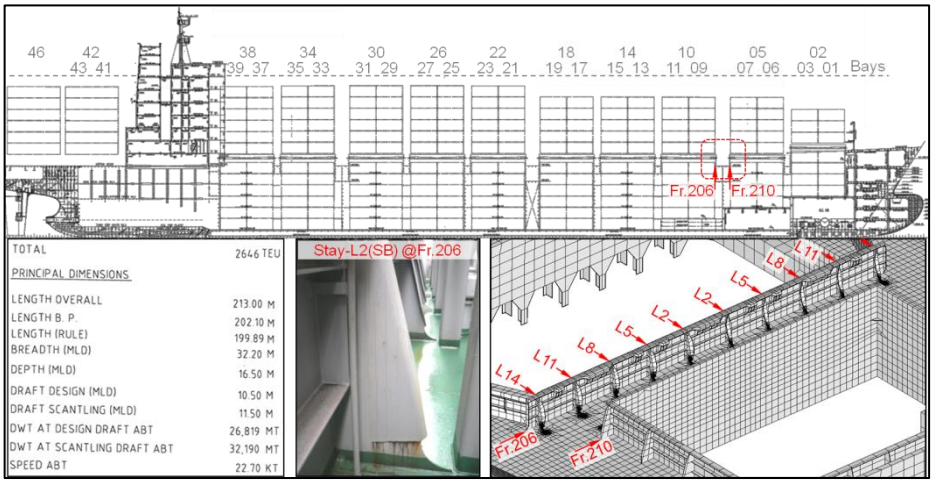

Fig. 1. Overview of the considered cracked transverse coamings stays in the vessel.

This study consists of three main sections. The first section presents a simplified methodology to validate the fatigue strengthening of the cracked stays. The second section presents the fatigue damage accumulation assessment conducted to validate the fatigue strengthening. The third section discusses on the crack driving loads, on the ship operational profile effect on the fatigue predictions and on the speed of the crack propagation.

2 Fatigue strengthening

2.1 Hot spot stress reduction factor

In practice, when a fatigue crack is detected in a structural detail, the most common corrective action consists in welding the crack [1] and thereby resetting the fatigue life of the structural hot spot. However, if the ship operational profile remains unchanged, the crack is expected to occur again after a period of time equivalent to the ship lifetime at the crack appearance (T_{crack}). For a crack occurring after half the ship design life (T_D), the welding repair might be deemed satisfactory since the cracking would not occur before the end of the design life. However, for a crack occurring before half the ship design life, the welding repair will not be sufficient to prevent the crack from reappearing within the design life. For that early cracking case, the redesign of the structural detail should be preferred in order to reduce the hot spot stress and, by then, increase its fatigue strength.

This section proposed a simplified approach to quantify the required hot spot stress reduction of the new structural detail design, so that its remaining fatigue life would at least meet the ship design life. The fatigue damage for a single slope S-N curve can be calculated with Eq.(1) as provided in IACS [2]. Although most of the S-N curves are doubly sloped, this single slope assumption of the S-N curve is deemed satisfactory in the case of an early crack appearance for which most of the fatigue damage is consumed in the low cycle part of the S-N curve.

$$D = \frac{N_D}{K_2} \cdot \frac{\Delta\sigma_{HS}^m}{(\ln N_R)^{m/\xi}} \cdot \Gamma\left(1 + \frac{m}{\xi}\right) \tag{1}$$

where $\Delta\sigma_{HS}$ is the long term hot spot stress range at the reference probability level of exceedance of $1/N_R$ that is set to 10^{-2} and a 2-parameter Weibul function $\Gamma(\,)$ with a shape parameter ξ taken as 1.0. K_2 and m are the S-N curve parameters, and N_D is the number of wave cycles experienced by the ship during the design fatigue life that can be expressed as:

$$N_D = f_0 \times T_D \times 365.25 \times 24 \times 3600/4\log(L) \tag{2}$$

where T_D is the ship design life, f_0 is the factor taking into account time in seagoing operations excluding time in loading and unloading, repairs, and L is the ship length.

For validating the fatigue strengthening, this study employed a simplified approach that expressed the ratio of target fatigue damage to achieve the remaining design life of the vessel (D_{target}) to the fatigue damage at the crack occurrence (D_{crack}) in the Eq.(3).

$$\frac{D_{target}}{D_{crack}} = \frac{N_{D,target} \times K_{2,o} \times \Gamma(1 + m_n)}{N_{D,crack} \times K_{2,n} \times \Gamma(1 + m_o)} \cdot \frac{\Delta\sigma_{HS,target}{}^{m_n} \times \left(\ln N_{R,crack}\right)^{m_o}}{\Delta\sigma_{HS,crack}{}^{m_o} \times \left(\ln N_{R,target}\right)^{m_n}} \tag{3}$$

where $K_{2,o}$ and m_o are the S-N curve parameters applicable to the hot spot of the original stay design and $K_{2,n}$ and m_n are the S-N curve parameters applicable to the hot spot of the new stay design, and where $\Delta\sigma_{HS,crack}$ and $\Delta\sigma_{HS,target}$ are the reference long-

term hot spot stress range at the probability level of $1/N_{R,crack}$ and $1/N_{R,target}$, respectively, that results in D_{crack} and in D_{target}, respectively, as calculated by Eq.(1).
, and with

$$D_{target} = T_D/(T_D - T_{crack}) \tag{4}$$

$$D_{crack} = T_D/T_{crack} \tag{5}$$

By assuming that the ship operational profile would remain unchanged after the crack repair and, by then, the long-term distribution of load cycles and loading conditions, the required hot spot stress range reduction to ensure a remaining life (T_D - T_{crack}) that meets the design life (T_D) can be calculated by Eq.(6).

$$\frac{\Delta\sigma_{HS,target}{}^{m_n}}{\Delta\sigma_{HS,crack}{}^{m_o}} = \frac{T_{crack}}{T_D - T_{crack}} \cdot \frac{K_{2,n} \times \Gamma(1+m_o)}{K_{2,o} \times \Gamma(1+m_n)} \cdot (\ln N_R)^{(m_n - m_o)} \tag{6}$$

In the case where the S-N curves applicable to the hot spots of the original and of the new design of the stays are the same, the Eq.(6) can be further simplified as expressed in Eq.(7):

$$\frac{\Delta\sigma_{HS,target}}{\Delta\sigma_{HS,crack}} = \left(\frac{T_{crack}}{T_D - T_{crack}}\right)^{1/m} \tag{7}$$

In the case where the S-N curves applicable to the hot spots of the original and of the new design of the stays are different, the reference hot spot stress range ($\Delta\sigma_{HS,crack}$) for a probability of exceedance of $1/N_{R,crack}$, here set to 10^{-2}, that results in a given damage of the original design (i.e. $D_{crack}=T_D/T_{crack}$) is to be deduced first as per Eq.(1), so that the target hot spot stress range can be evaluated as expressed in Eq.(8).

$$\Delta\sigma_{HS,target} = \left(\frac{T_{crack}}{T_D - T_{crack}} \cdot \frac{K_{2,n} \cdot \Gamma(1+m_o)}{K_{2,o} \cdot \Gamma(1+m_n)} \cdot \left(\ln N_{R,crack}\right)^{(m_n - m_o)} \cdot \Delta\sigma_{HS,crack}{}^{m_o}\right)^{\frac{1}{m_n}} \tag{8}$$

, and the hot spot stress range reduction factor formulation in Eq.(6) becomes Eq.(9).

$$\frac{\Delta\sigma_{HS,target}}{\Delta\sigma_{HS,crack}} = \left(\frac{T_{crack}}{T_D - T_{crack}} \cdot \frac{K_{2,n} \times \Gamma(1+m_o)}{K_{2,o} \times \Gamma(1+m_n)} \cdot \left(\frac{\Delta\sigma_{HS,crack}}{\ln N_{R,crack}}\right)^{(m_o - m_n)}\right)^{\frac{1}{m_n}} \tag{9}$$

For the original stay, the crack initiated from a hot spot located at the edge of a machine-cut soft toe. The FAT125 S-N curve with a slope set to m=3.5 is appropriate for this type hot spot to evaluate the fatigue damage as provided by the IACS [2] based on IIW recommendation [3]. A first fatigue strengthening strategy has consisted in increasing the soft toe radius and consequently, the same FAT125 (m=3.5) S-N curve was thus applicable. Another fatigue strengthening strategy was considered in line with IACS recommendation [4] that consisted in adding a face plate at the edge of the stay, so that the hot spot would now be located at the welded joint between the face plate and the deck. Consequently, the FAT90 (m=3.0) S-N curve was selected because commonly used for the fatigue assessment of welded connections by using the

stress interpolation technique [0.5t; 1.5t] as provided by IACS [2] based on Maddox [5] study. Fig. 2 illustrates the S-N curve FAT125 (m=3.5) and FAT90 (m=3).

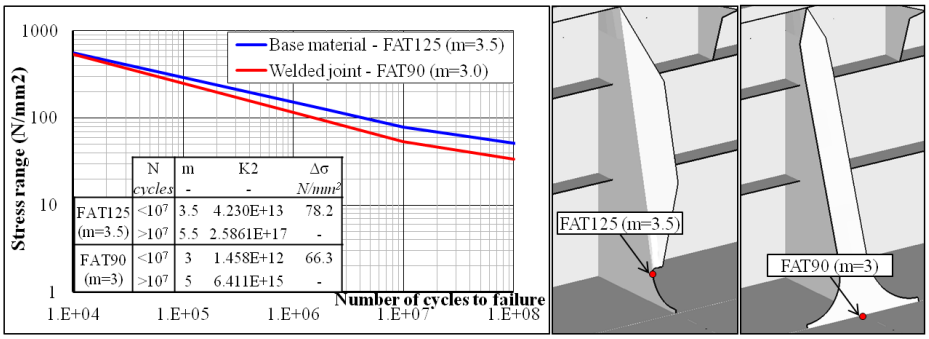

Fig. 2. S-N curves applicable to the fatigue assessment of the original and the fatigue-strengthened stay.

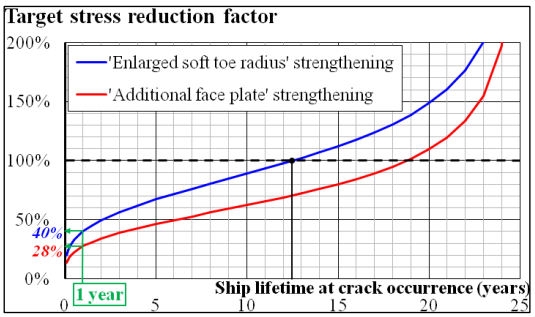

Fig. 3. Target hot spot stress reduction factor to be achieved by the fatigue strengthening.

Then, the target stress reduction factor for crack occurrence at various ship lifetimes was evaluated as per Eqs.(7) and (9) for the two fatigue strengthening strategies, as shown in Fig. 3. It can be observed that, for the 'Enlarged soft toe radius' strengthening, the target stress reduction factor was approximately 13% larger than that produced for the 'Additional face plate' strengthening, and as such, this first strategy looked more efficient to strengthen the stay against fatigue cracking. Over all the considered ships, the earliest crack occurred after 1.0 year operation. Therefore, to produce accordingly a satisfactory strengthening against fatigue cracking, the target hot spot stress reduction factor to be achieved by the new stay design should be approximately of 40% for a redesign involving a larger soft toe radius, or 28% for a redesign involving an additional welded face plate.

2.2 Hot spot stress reduction evaluation

This study employed finite element analyses (FEA) to evaluate the hot spot stress reduction between the original and the redesigned stays. For that, an identical nominal loading condition will be applied on both stays FE model, so that the produced hot spot stresses can be consistently compared. For those FE analyses, the orientation of the load must reflects the realistic load configuration that maximized the stress at the hot spot and, as such, contributed the most to the fatigue. For the hatch cover ultimate strength assessment, the IACS [6] requires to consider that the on-deck containers longitudinal component of the inertia loads transmitted to the hatch cover is carried by the stoppers, while the bearing pads, thereby assumed frictionless, would only transfer the vertical component of the inertia loads. However, in Fig. 1, the orientation of the crack path helped identifying the direction of the principal stresses driving the fatigue that, by definition for a mode I of crack opening, are perpendicular to the crack direction. This crack orientation was thus induced by an in-plane bending of the stay driven by the longitudinal inertia load fluctuations transmitted from the hatch cover to the top of the transverse coaming, so that non-negligible friction forces were transmitted through the bearing pads. Likewise, the IACS [4] provides several recommendations for the strengthening of transverse hatch coaming stays that suffered fatigue cracking, and identifies the source of the damage as being due to an *"insufficient consideration of the horizontal friction forces in way of the bearing pads for hatch cover"*. Finally, it worth being noted that, as located inside the line of hatch opening, the stays are not exposed to the global bending and torsion of the hull girder, and those effects were here disregarded accordingly.

In addition, the IACS requirements [6] for the hatch covers ultimate strength evaluation provide design loads that, at the considered foremost container bays (see Fig. 1), set an extreme cyclic heave acceleration amplitude of 0.45 g's and a longitudinal acceleration of 0.2 g's. The combination of those vertical and longitudinal accelerations was thus used in this study as a first estimate to determine the orientation of the crack driving loads, here set to $F_x = 44\%F_z$, to be applied for the hot spot stress reduction assessment.

The stays local FE models were then made of shell elements with a very fine mesh size set to the plating thickness, so called *'t× t'*, and the steel material represented as linear elastic. Fig. 4 shows the Finite Element models of the original stay and those of the strengthened stay designs. This model was deemed small enough to be rapidly built and sufficiently large to reduce the effect of the boundary conditions on the hot spot stress. Finally, a nominal load with an orientation of $F_x = 44\%F_z$ was applied at the top plate in way of the stay, where the bearing pads are located, and an amplitude arbitrarily set so that, for the original stay, a hot spot stress of 100 N/mm^2 was obtained that enabled a clearer observation of the stress reduction factor (%) achieved by the strengthened stay designs.

All the strengthened stay designs employed the same 11 mm mild steel plating as for the original design, so that new hot spots would not arise by mounting stays significantly stiffer than the adjacent hatch coaming structural members. Fig. 4 shows, for the various designs of stay, the main modifications and the resulting hot spot stress

produced by FEA. It can be observed that by enlarging the soft toe radius to 400 mm, the hot spot stress reduction factor (92%) did not meet the target value of 40% (see Fig. 3), whereas by adding a face plate, the hot spot stress reduction factor of 'FP2' (27%) did meet the target value of 28%. In addition, as recommended by the IACS [4] to improve the fatigue strength, a full penetration butt-weld was provided at the face plate connection to the deck.

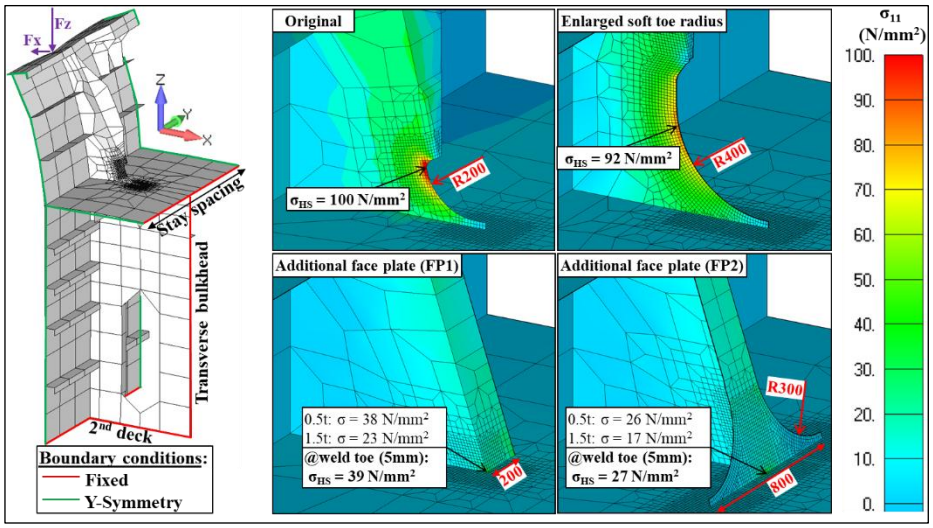

Fig. 4. Local FE model of the Stay-L2 at Fr.206 (left) and hot spot stress reduction assessment for the strengthened designs (right).

3 Fatigue life assessment

3.1 Ship operational profile

The 6 sister vessels were chartered on a North Pacific route between Taipei and Los Angeles with a time in seagoing condition corresponding to 80% of their operations. The average speed was set to 80% the vessel design speed of 22.7 knt and two loading conditions were considered by this study corresponding to 75% and 100% the total deadweight capacity. Table 1 lists the ship hydrostatic properties for those two loading conditions. The actual on-deck containers loading conditions of the foremost bays were not made available, but the loading manual indicated that, between 75% to 100% the total design capacity, the on-deck container mass distributions at those bays would be identical with an average mass of 24 t per 40' containers. For this study, it was thus assumed that the bays were commonly fully loaded. Table 2 lists the details of the related on-deck container bay arrangement.

Table 1. Ship hydrostatic properties.

	75% DWT	100% DWT
Displacement (t)	40516.1	45880.8
LCG (m)	98.32	97.54
VCG (m)	13.88	14.49
Draft - MS (m)	10.48	11.42
Trim (deg)	0.27	0.53

Table 2. Foremost bays' containers arrangement on hatch covers.

Bays (see Fig. 1)	14 15 13	10 11 09	06 07 05	02 03 01
Containers arrangement on hatch covers	4 Tiers × 11 Rows	4 Tiers × 11 Rows	4 Tiers × 7 Rows	2 Tiers × 5 Rows
Mass of bay (t)	1056	1056	672	240
XG (m)	140.6	154.7	170.5	184.6
ZG (m)	24.4	24.4	24.4	24.5

3.2 Ship motions and structure analyses

The structural model of the foremost hatches was made of shell elements with a mesh size set to the stiffener spacing (here ~600 mm) and the steel material was represented as linear elastic. In addition, at the hotspots, the transverse coaming stays on Fr.206 and Fr.210 were represented using the very fine mesh *'t× t'* technique previously described in section 2.2. Fig. 5 shows the Finite Element model of the foremost hatches that extended vertically from the 2nd deck, with the container mass carried by the corresponding hatch covers represented through mass elements (red squares) located at the center of gravity provided in Table 2, and the interpolation elements (blue lines) that were employed to distribute the inertia loads from the mass elements to the corresponding hatch covers bearing pads. Finally, the aft and fore ends of the model, as well as the 2nd deck were set as simply supported. Though bigger than the local models presented in Fig. 4, this model was deemed small enough to be rapidly built and sufficiently large to reproduce realistically the inertia loads distribution on the hatch coaming and to reduce the effect of the boundary conditions on the hot spot stress. In addition, the sliding of the hatch cover was here disregarded, as discussed in section 2.2, by the use of the interpolation elements that transmitted the whole of the longitudinal component of the inertia loads through the bearing pads.

A first FE model was created based on the original design of the stays, and then a second version was made by replacing the critical stays-L2, -L5 and -L8 at Fr.206 by the strengthened stay design 'FP2' presented in Fig. 4. The structural response was evaluated by static analysis conducted with NX NASTRAN [7] and the loads in terms of ship motions and accelerations were transferred from seakeeping analyses carried out through Hydrostar [8].

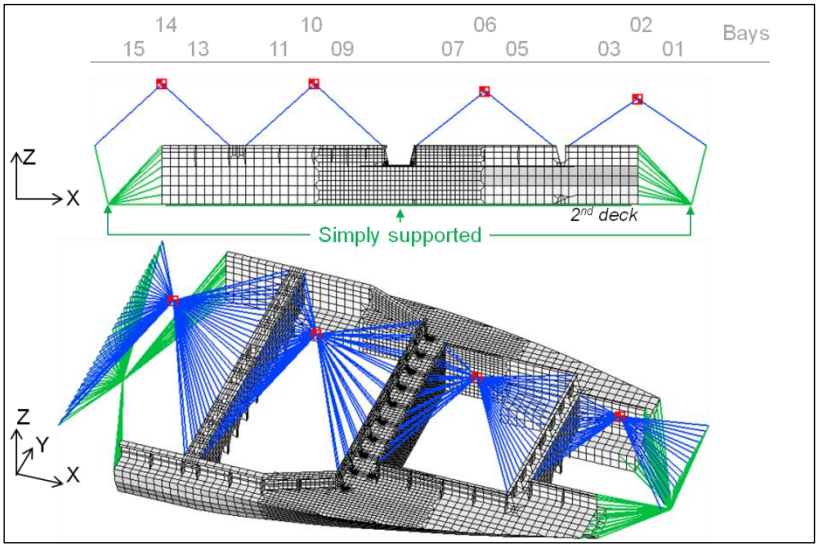

Fig. 5. Foremost hatches FE model.

First, the structural response in stillwater condition was evaluated by FEA. Table 3 lists the mean stress at the hot spots of each stay that appeared to be always in tension since this loading condition resulted in the inward deflection of the transverse hatch coamings at Fr.206 and Fr.210. The mean stress effect was thus disregarded in the next fatigue life assessment, since it is especially relevant for compressive mean stress.

Table 3. Hot spot mean stress at the transverse coaming stays.

σ_{mean} (N/mm^2)	Fr.206					Fr.210		
	L2	L5	L8	L11	L14	L2	L5	L8
Original stays	34.5	20.3	25.5	8.8	-16.4	25.5	11.8	9.9
Strengthened stays	19.8	16.6	15.2	-	-	-	-	-

The seakeeping analyses were then carried out using the potential flow theory CFD software Hydrostar [8] for the two considered loading conditions (see Table 1). The ships motions were evaluated for 36 wave headings from 0° to 350° and for 40 wave frequencies from 0.05 rad/s to 2.0 rad/s. Fig. 6 shows, for both loading conditions, the produced response amplitude operators (RAO) of ship heave acceleration and pitch motions. It appeared that the largest motions were obtained for the head sea (here, h=180deg) and quartering seas, and that the largest motions were induced for the loading condition set to 75%DWT. Therefore, since the foremost bays' hatch covers carried the same on-deck container mass for both loading conditions, the inertia loads produced by the 75%DWT motions will be larger than for that of the 100%DWT, and, accordingly, the fatigue lives obtained for the 75%DWT motions were anticipated to be the lowest.

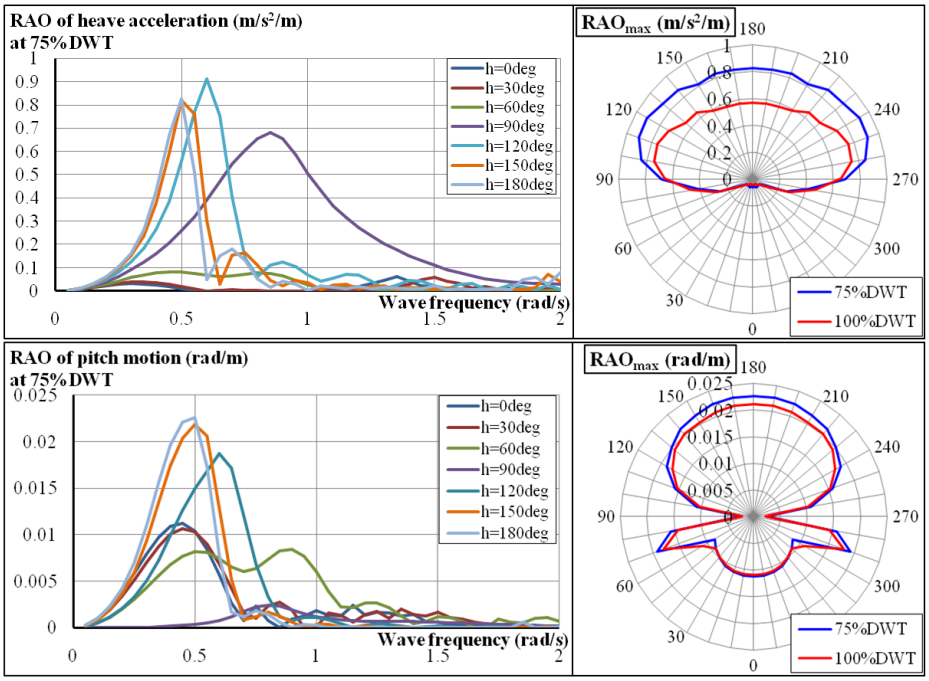

Fig. 6. RAOs of ship heave acceleration (top) and pitch motion (bottom) and corresponding peak values' wave heading distribution.

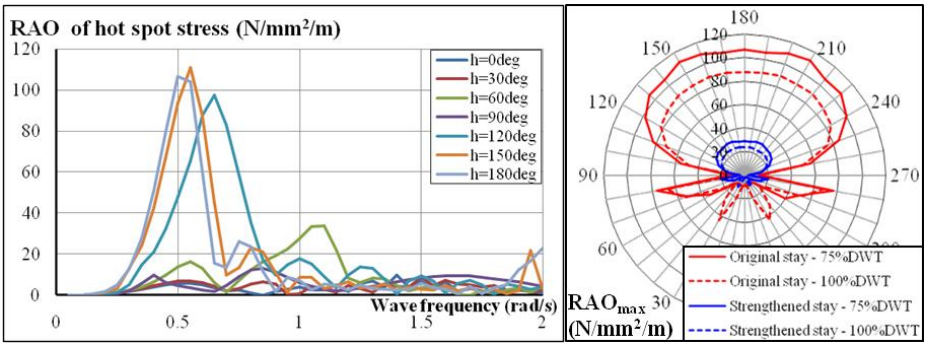

Fig. 7. RAO of hot spot stress of the original stay-L2 at Fr.206 for 75%DWT (left), and corresponding peak values' wave heading distribution for the original and the strengthened stays for loading conditions set to 75%DWT and 100%DWT (right).

After transferring the loads to both the original and the strengthened stays FE models, the finite element analyses were conducted and the RAO of hot spot stress were then extracted as needed for the spectral fatigue assessment. Fig. 7 (left) shows the RAOs of hot spot stress of the stay-L2 at Fr.206 for a loading condition set to 75%DWT, and (right) the corresponding peak values of the original and the strengthened stays for

loading conditions set to 75%DWT and 100%DWT. It can be observed that the largest stress RAOs occurred in head (here, h=180deg) and quartering sea, while rapidly dropping for beam sea and beyond until following sea (here, h=0deg). It appeared also that, for the strengthened stay, the peak values dropped significantly compare to those of the original stay, up to 3.6 times decrease for the head sea and both loading conditions.

3.3 Fatigue damage accumulation

Spectral fatigue analyses (SFA) were conducted to evaluate the fatigue damage for 25 years of seagoing operations. The 3-hour short-term stationary irregular sea states was described by a Pierson-Moskowitz wave spectrum combined to a cosine 2s wave spreading spectrum as recommended by IACS [9] to represent a fully-developed sea that corresponds to most of the sea-states encountered by the vessels. For the North Pacific route (i.e. 'Taipei to Los-Angeles') on which the ships were chartered, and the South China Sea route (i.e. 'Taipei to Singapore') on which the ships is presently chartered (see Fig. 8), the long-term wave environments were derived from the wave scatter diagrams provided by the Bmt [10] for various ocean areas. The equivalent wave scatter diagram was produced as the sum of the scatter diagrams corresponding to the ocean areas crossed by the ships along the shortest path and weighted by the fraction of time in each area which was taken as the ratio of the crossed distance in each area to the total distance. The encountered wave headings were taken as uniformly distributed. This approach disregarded thus the effect of the speeds and heading variations induced by the routing under weather and operations constraints. Finally, the S-N curves presented in Fig. 2 were used to evaluate the accumulated fatigue damage of the original and the 'FP2' fatigue-strengthened stays (see Fig. 4).

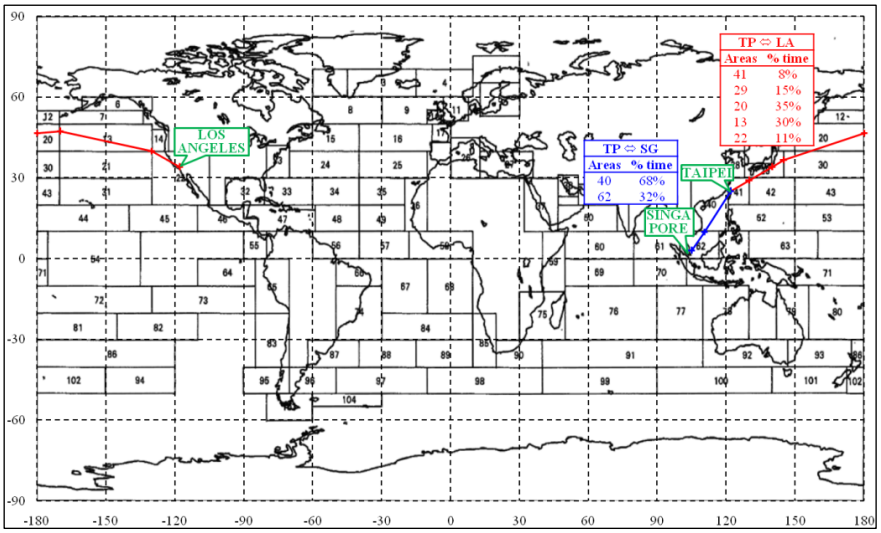

Fig. 8. Considered trading routes drawn on Bmt's *'Map of Area Subdivisions'* [10].

Table 4. Evaluated fatigue life of the stays for the North Pacific route.

		Fr.206					Fr.210		
		L2	L5	L8	L11	L14	L2	L5	L8
75%DWT	Original stay (years)	0.4	0.2	0.9	14.2	>50yrs	1.2	0.8	2.2
	Strengthened stay (years)	14.6	4.7	27.3	-	-	-	-	-
	Strengthened/Original (-)	**36.5**	**23.5**	**30.3**	-	-	-	-	-
100%DWT	Original stay (years)	0.8	0.3	1.8	20.4	>50yrs	2.5	1.4	3.5
	Strengthened stay (years)	30.6	9.0	53.4	-	-	-	-	-
	Strengthened/Original (-)	**38.3**	**30.0**	**29.7**	-	-	-	-	-

Table 4 lists the evaluated fatigue life of each stay for the two loading conditions and the North Pacific route long-term wave environments. It can be observed that the most critical fatigue life was obtained for the hot spot of the stay-L5 supporting the transverse hatch coaming at the Fr.206 with a fatigue life comprised between 0.2 and 0.3 years for loading conditions set to 75% and 100% the deadweight capacity, respectively. The evaluated fatigue lives were thus significantly lower than the 1.0 years actually observed in terms of cracking on board those ships. Those large deviations with the observations can be explained by the lack of operation data needed to produce a realistic fatigue assessment, especially the typical loading conditions and associated on-hatch-cover container mass distribution, and possibly the weather and operation routing constraints. Likewise, the evaluated fatigue of the strengthened stay-L5 only reached 4.7 and 9.0 years for loading conditions set to 75% and 100% the deadweight capacity, respectively. However, the fatigue strengthening can be validated based on the fatigue strengthening ratios of the evaluated fatigue life produced for the strengthened stays to that obtained for the original stays. In section 2, the target fatigue strengthening ratio was of 24 (i.e. a fatigue life increase from 1 year at the observed cracking to 24 years to achieve the remaining design life). In Table 4, it appeared that, for both loading conditions, the minimum fatigue strengthening ratio was of 23.5 (L5 at 75%DWT) and reached 38.3 (L2 at 100%DWT). Therefore, the fatigue strengthening was satisfactory and the simplified approach presented in section 2 to confirm the fatigue strengthening was thus validated by the predictions of the spectral fatigue analyses.

4 Discussions

4.1 Fatigue driving loads

Fig. 9 shows the fatigue damage distribution of the original stay-L2 at Fr.206 as it relates to the wave heading (left) and to the probability level of loads (right). It can be observed that the maximum damage contribution was produced for the head sea (here, 0 deg) and for long-term loads with a probability level of approximately 10^{-2}. An equivalent design wave (EDW) was thus derived from the RAO of hot spot stress in

head sea (see Fig. 7, h=180deg) with a long-term value at a probability level of 10^{-2}. Table 5 lists the EDW parameters.

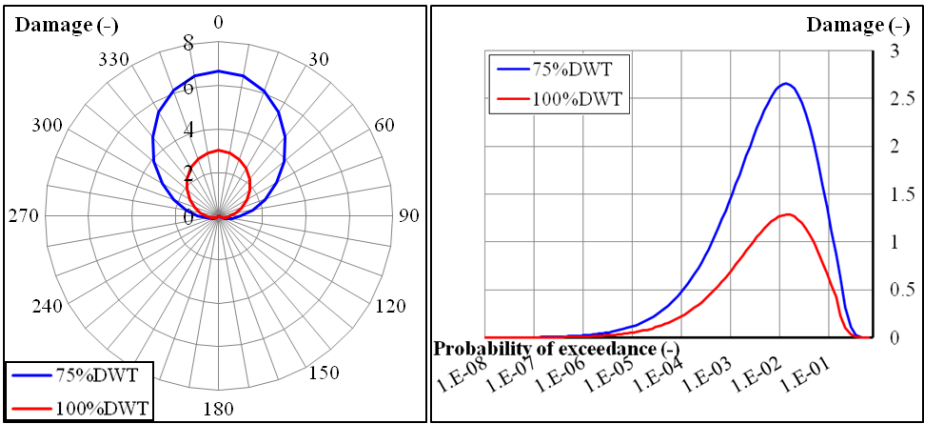

Fig. 9. Fatigue damage distribution vs. wave heading (left) and vs. probability level of loads (right) for the stay-L2 at Frame206.

Table 5. Equivalent design wave maximizing the hot spot stress.

Loading conditions	Long-term hot spot stress range at a P=10-2	Wave heading (RAO)	Peak value and associated wave frequency of RAO of hot spot stress		EDW amplitude $= \frac{LT\_\Delta\sigma HS}{2 \times RAO\_\sigma HS,\,max}$
	$LT\_\Delta\sigma_{HS}$	h	$RAO\_\sigma_{HS,max}$	ω_{max}	A_{EDW}
	N/mm²	*deg*	*N/mm²*	*rad/s*	*m*
75%DWT	316	180	107	0.50	1.48
100%DWT	263	180	87	0.55	1.51

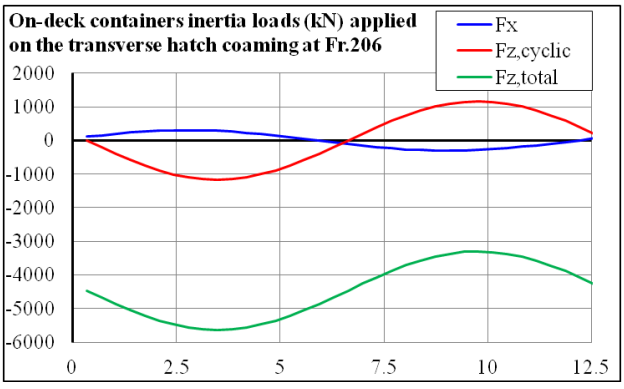

Fig. 10. Evolution over one EDW period of the on-deck containers load applied on the transverse hatch coaming at Fr.206.

Fig. 10 shows the corresponding evolution, over one EDW period, of the on-deck containers inertia loads applied on the transverse hatch coaming at Fr.206. It appeared that the longitudinal component of the applied inertia loads (F_x), at its extremes, was 28% as large as the cyclic part of the vertical component of loads ($F_{z,cyclic}$; here disregarding the static weight), that is significantly lower than the load ratio of 44% derived from the IACS recommendation in section 2.2. In addition, it can be observed that F_x, at the extremes, fluctuated between 5% and 10% the whole of the vertical component of loads ($F_{z,total}$; here considering the static weight) that is of the same order as the coefficient of friction of 0.1 for the steel-steel contact in dry condition as provided by the IMO [11]. It can be argued that the coefficient of friction of the bearing pads that are made of specific steel alloys (here, Hardox® [12]) to reduce the abrasion and thus the friction, should be lower than 0.1. Therefore, the foremost hatches FE model (see Fig. 5) would generate conservative results by transmitting the whole of the longitudinal component of the inertia loads acting on the hatch cover, whereas it should be limited by the sliding.

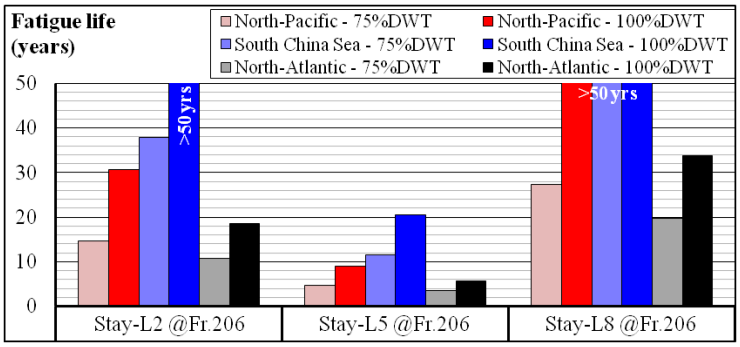

Fig. 11. Evaluated fatigue life of the strengthened stays.

4.2 Wave environments

After the stays upgrade, the vessel continued operating on the North Pacific route for about 2 years before being redirected to a South China Sea route for the last 6 years, and yet no crack has been detected, thereby comforting the effectiveness of the strengthening. Fig. 11 shows the evaluated fatigue of the strengthened stays for the two trading routes. It can be observed that the evaluated fatigue life produced for the South China Sea route was approximately 2.5 times that obtained for the North Pacific route. Therefore, it is believed that the combined actions of strengthening and milder wave environment will prevent any crack from reoccurring before the end of the design life. However, it can also be observed that the evaluated fatigue lives produced for the North Atlantic wave environment, commonly considered by the Class rules for unrestricted operations, were approximately 0.6 times that obtained for the North Pacific route, thereby reducing the fatigue strengthening ratios listed in Table 4 to 14.1 (L5 at 75%DWT) and 23.0 (L2 at 100%DWT) that would be less than the target

ratio of 24 (i.e. increase the 1.0 year fatigue life to the 24 years remaining design life). Therefore, for North Atlantic operations, the present strengthening would not have been sufficient. The definition of the trading route and the associated weather and operation routing can thus greatly influence the fatigue life and the assumption of unchanged operational profile made in section 2.1 for assessing the fatigue strengthening must be carefully considered when using this approach.

4.3 Crack propagation

As mentioned in Introduction, the crew reported that, under severe conditions, ~50 mm long cracks appeared in the considered stays after a voyage lasting approximately 1 week. This study evaluated the crack propagation from an undetected level of crack length, here arbitrarily set to 5 mm, until the length of 350 mm observed in Fig. 1. For that, the crack was idealized as a sharp tipped crack that propagated at a crack growth rate calculated by Eq.(10).

$$\frac{da}{dN} = A(\Delta K)^m \tag{10}$$

where ΔK is the stress intensity factor range evaluated at the tip of the crack of length a, and A and m are constants that depends on the material and the applied conditions including environment and cyclic frequency. Fig. 12 shows the crack growth law and the associated constants recommended by British Standard [13] for unwelded steels and operations in air as ensured by the protective coating good condition of the stays (see Fig. 1).

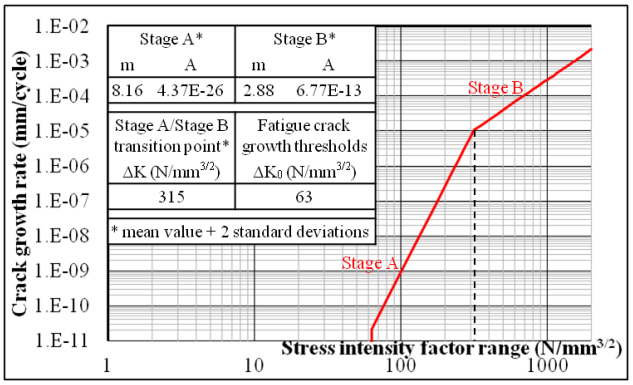

Fig. 12. Fatigue crack growth law for unwelded steel and in air environment.

The stress intensity factor was evaluated by finite element analyses conducted on a local finite element model of the stay including a crack as shown in Fig. 13. The initiation point and the direction of the crack were defined accordingly to that observed in Fig. 1. The cracked stay FE model was made of quadrilateral shell elements with centered nodes, referenced as S8R5 in Abaqus [14]. The meshing produced concentric

rings of element centered on the crack tip. The elements in the innermost ring were then degenerated to triangles by merging the three nodes of one S8R5 element edge as provided by Abaqus to extract stress intensity factor as per the linear elastic fracture mechanic formulation.

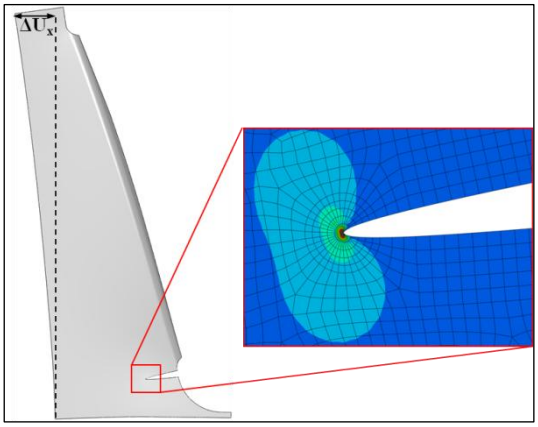

Fig. 13. FE model of the original stay including a 150 mm long crack.

Besides, the crack propagation is a nonlinear process that highly depends on the loads history. A realistic approach would consist in simulating the crack propagation for various sequences of severe sea-states actually observed on the considered route. However, the present study proposed to employ the statistical long-term load distribution produced by the spectral fatigue analysis previously described in section 3.3. The method consisted then in scaling the 25-year long-term load distribution down to a 1-week load cycles block where the amplitude of the loads will increase during 3.5 days and decrease during the remaining 3.5 days, thereby reproducing in a statistical manner a 'calm-severe-calm' weather sequence met during a voyage. The 1-week load cycles block was then repeated until the crack met the target length of 350 mm. Therefore, for various crack lengths, the RAOs of stress intensity factor was obtained using a top-down scheme that applied the nodal displacements at the boundaries of the stay-L2 (see Fig. 13) previously produced by the FEA of the foremost hatches FE model (see Fig. 5) for each wave heading and frequency. A spectral analysis was then conducted to obtain the long-term distribution of stress intensity factor range. The load cycles block construction was then simplified by dividing the long-term distribution of the stress intensity factor range (ΔK) for each crack length by that of the stay deflection range (ΔUx, see Fig. 13) that resulted in a stress intensity factor per mm of stay deflection (K/Ux) which the evolution as a function of the crack length was unified for any level of loads with a very good precision as shown in Fig. 14 (right). The 1-week load cycles block construction (see Fig. 14, middle) was thus derived from the long-term distribution of stay deflection range (see Fig. 14, left).

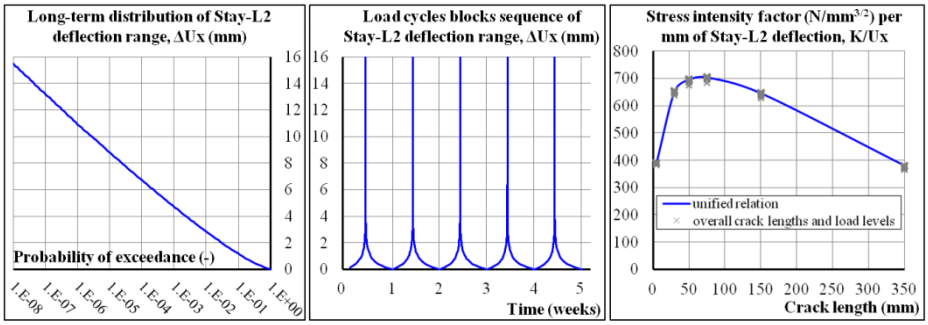

Fig. 14. Long-term distribution of stay-L2 deflection (left) and the associated 1-week load cycles blocks sequence (middle), and the stress intensity factor relation to the crack length (right).

The crack growth was then evaluated as per Eq.(10) at every load cycle illustrated in Fig. 14 (middle). Fig. 15 shows the evaluated crack growth and the corresponding weekly crack growth rate for various wave environments, when assuming an initial undetected crack length of 5 mm. For the North Pacific route wave environment, it appeared that a 50 mm crack length was reached after simulating approximately 8 weeks of operations for both loading conditions. Those predictions can only be considered as the average crack propagation prediction over a sufficiently large period and not as the realistic status of the crack length at a specific time. Especially, during the first 75 mm of the crack propagation, the weekly crack growth rate varies rapidly. It can thus be argued that if the vessel had encountered successive or extensive severe weather conditions within a concentrate period that corresponds to the beginning of the crack propagation, the crack growth would have been much accelerated, and a 50 mm to 100 mm crack could appear within 1 to 2 weeks as previously observed by the crews. The use of a more realistic storm model such as that recommended by DNVGL [15] calibrated on actual seasonal data would be necessary to further discuss on the crack propagation. However, it can already be confirmed that the integrity of this kind of structural detail can be dangerously and rapidly compromised if the fatigue damage is not correctly taken into account at the design stage.

Besides, in Fig. 15, it can be observed that, contrary to the fatigue damage, the ship loading conditions had a limited effect on the fatigue crack growth, whereas the considered wave environment still had a significant influence on the predictions. Finally, with respect to the strengthened stay 'FP2', it is anticipated that the face plate will intrinsically greatly reduce the potential crack propagation rate since there would be three crack-tips to resist to the crack growth (i.e. one in the stay plus two in the face plate propagating on each side of the stay along the weld with the deck) instead of one crack-tip for the original design.

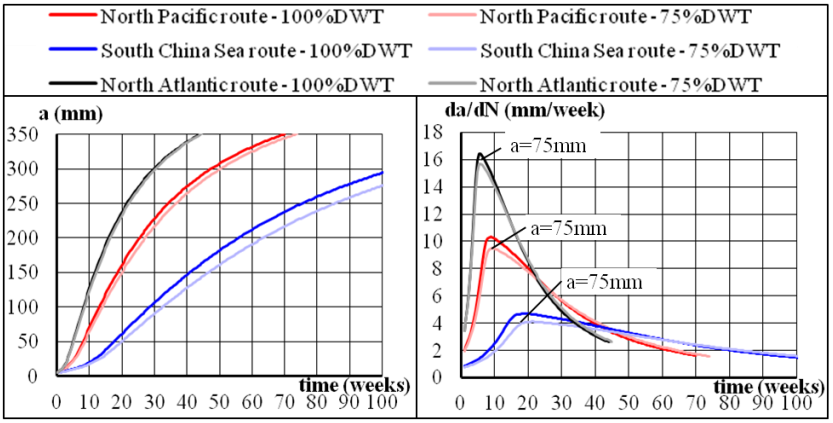

Fig. 15. Evaluated crack growth (left) and the corresponding weekly crack growth rate (right) for various wave environments and ship loading conditions.

5 Conclusions

This study evaluated the fatigue strengthening of the transverse hatch coaming stays of 6 sister container vessels that suffered cracking after 1.0 year operation on a North Pacific route. At first, this method proposed a simplified method to validate the fatigue strengthening by providing a target hot spot stress reduction factor relating to the ship lifetime at the crack occurrence. This method assumed that the operational profile of the ship remained unchanged after the stay upgrade, that consisted in adding a face plate at the edge of the stays, and considered in view of the crack orientation that a non-negligible part of the longitudinal component of the on-deck container inertia load was transferred through the hatch covers' resting pads that are commonly considered as frictionless. Then, spectral fatigue assessment (SFA) were conducted by transferring the ship motions and accelerations on two FE models of the foremost hatches that included separately the original and the strengthened design of stays. The produced fatigue lives of the original stays were approximately of 0.2 years and as such did not reflect the observed fatigue life. However, the produced fatigue strengthening ratio of the fatigue life obtained for the strengthened stays to that produced for the original stay matched the target defined for the simplified method, thereby validating the accuracy of this approach.

The detail examination of the SFA calculations showed that the assumptions made for the simplified method in terms of dominant fatigue driving loads were relevant. However, the SFA and crack propagation results showed also that the fatigue life assessment were very sensitive to the considered loading condition and the wave environment, so that more information would be needed to improve the accuracy of the fatigue life predictions. Besides, it appeared that the proper consideration of the coefficient of friction of the hatch covers' bearing pads would also have a significant effect on the fatigue evaluation by limiting the inertia loads transmitted by friction from the hatch cover to the corresponding transverse coaming. Finally, crack growth as-

sessments confirmed the criticality of the stays to the fatigue cracking when the fatigue damage is not appropriately considered at the design stage.

References

1. IACS: Shipbuilding and Repair Quality Standard - Part B. Repair Quality Standard for Existing Ships, Recommendation No. 47 (2017).
2. IACS: Common Structural Rules for Bulk Carriers and Oil Tankers - Pt.I Ch.9, CSR (2018)
3. Hobbacher, A.: Recommendations for Fatigue Design of Welded Joints and Components, IIW doc. 1823-07, Welding Research Council Bulletin 520, New York (2009).
4. IACS: Container Ships - Guidelines for Surveys, Assessment and Repair of Hull Structures - Example No. 12-a, Recommendation No. 84 (2017).
5. Maddox, S.J.: Recommended Hot-Spot Stress Design S-N Curves for Fatigue Assessment of FPSOs, Proceedings of the Eleventh International Offshore and Polar Engineering Conference, Stavanger, Norway, (2001).
6. IACS: Evaluation of Scantlings of Hatch Covers and Hatch Coamings and Closing Arrangements of Cargo Holds of Ships, Unified Requirement concerning the strength of ships, UR-S21A (2011).
7. NX NASTRAN, www.plm.automation.siemens.com, last accessed 2019/03/04.
8. Hydrostar, www.veristar.com, last accessed 2019/03/04.
9. IACS: Standard Wave Data, Recommendation No. 34 (2001).
10. Hogben, H., Dacunha, N.M.C., Olliver, G.F.: Global wave statistics, British Maritime Technology Limited, Teddington, UK (2000).
11. IMO: Code of safe practice for Cargo Stowage and Securing (CSS Code), London (2002).
12. SAAB: www.ssab.fr/products/brands/hardox, last accessed 2019/03/04.
13. British Standard: Guide to methods for assessing the acceptability of flaws in metallic structures, BS 7910 (2015).
14. Abaqus: www.3ds.com, last accessed 2019/03/04.
15. DNVGL: Environmental conditions and environmental loads, RP-C205 (2017).